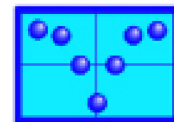


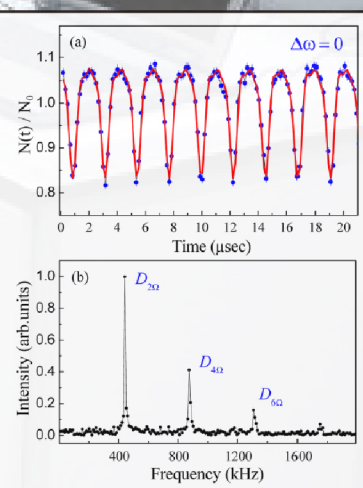
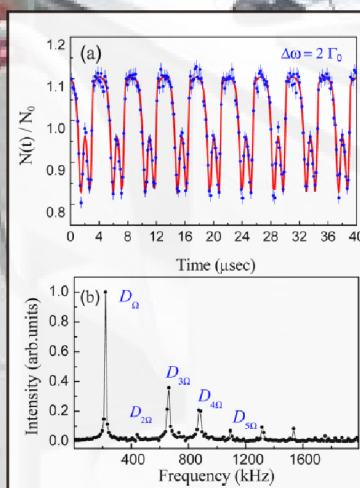
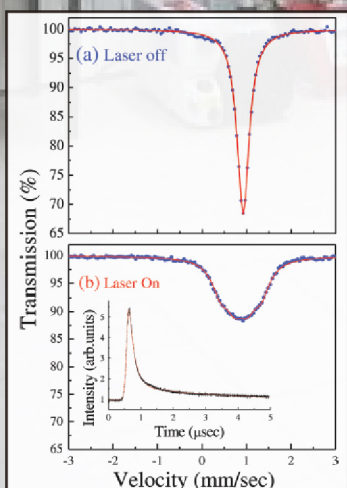
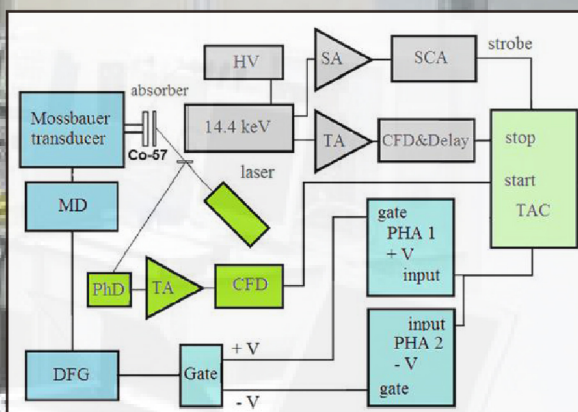
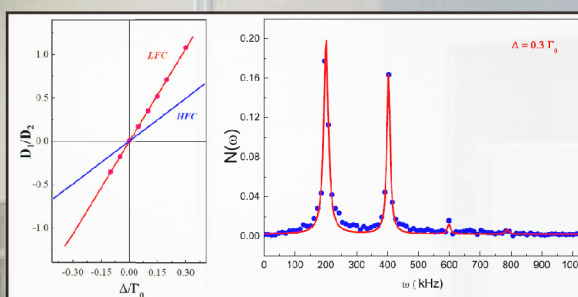
# Mössbauer Effect

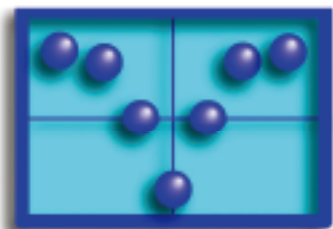
## Reference and Data Journal



August 2020 • Volume 43 • Number 6

### *New application of the Mössbauer effect*





# MÖSSBAUER SPECTROSCOPY NEWSLETTER

August 2020

## New application of the Mössbauer effect I. Modulation effects

F. G. Vagizov<sup>1,2</sup> (✉), R. N. Shakhmurov<sup>1,3</sup>,  
O. Kocharovskaya<sup>2</sup>

<sup>1</sup>Institute of Physics, Kazan Federal  
University, Kazan, Russia

<sup>2</sup>Department of Physics and Institute for  
Quantum Studies, Texas A&M University, USA

<sup>3</sup>Kazan Physical-Technical Institute,  
Russian Academy of Science, Kazan, Russia  
Email: vagizovf@gmail.com

### Abstract

In this short review, we present the results of some experimental research on the somewhat unusual applications of the Mössbauer effect in the field of modulation and quantum interference effects. Based on the results of experiments carried out in recent years at Kazan Federal University and the Texas A&M University, we will show that the extremely high Q-factor of Mössbauer transitions for some isotopes and the presence of a cascade scheme of their decay can significantly increase the accuracy of Mössbauer measurements of small periodic displacements induced by acoustic oscillations, and open up the possibility of developing methods of coherent control of the shape of single-photon wave packets using resonant absorbers.



**Farit Vagizov** is an Associate Professor of Physics at the Kazan Federal University, Russia. He obtained his Ph.D. in Solid State Physics from Kazan State University in 1989. One of his works devoted to the ultrasonic modulation of Mössbauer radiation was recognized as outstanding achievement of Russian Academy of Sciences in the field of acoustical physics. Prof. Vagizov has been carrying out experimental research with emphasis on Mössbauer effect study of condensed matter systems: intermetallic compounds, hard magnetic materials and gamma optics during the last years.



**Rustem Shakhmurov** graduated and received his Ph.D. from Kazan State University, Russia. He has been involved in theoretical studies, related to various aspects of Physics: the resonant interaction of coherent radiation with solids, relaxation processes of optical coherence and of spin (electron and nuclear) coherence, dynamical processes in lasers and lasers without inversion, gamma-optics. He studied coherent transients in solids in collaboration with the Institute for Microstructural Studies, National Research Council of Canada, Ottawa, and with the University of Palermo, Italy. He has been involved in research in gamma-optics with the Katholieke Universiteit Leuven, Belgium. His current interests cover electromagnetically induced transparency, slow light phenomena and storage of quantum information.



**Olga Kocharovskaya** is Distinguished Professor of Physics at the Texas A&M University. She graduated and received Ph.D. from Gorky State University (now Nizhny Novgorod), Russia. Olga Kocharovskaya's research is focused on Quantum, Coherent and Nonlinear Optics, Quantum Information Science, Attosecond Physics and X-ray Optics. She made pioneering contributions on Electromagnetically Induced Transparency, Lasing Without Inversion and Coherent Control of the Nuclear Transitions. She received many the Distinguished Scientist Award of the Texas A&M University, Willis Lamb Award for achievements in laser science and quantum electronics.

### Introduction

Mössbauer spectroscopy is a unique technique for investigating structural and dynamical properties of solids on the atomic scale. This technique provides information about local symmetry, magnetic ordering, and chemical bonding in the immediate vicinity of the probing nucleus. Among many other promising applications of Mössbauer effect there are those, which provide information about dynamical processes induced in materials by radiofrequency (RF) magnetic field, ultrasound, and optical laser radiation [1]. Since the discovery of the Mössbauer effect a number of interesting phenomena stimulated by external fields were observed: Ultrasonic [2] and magnetostriction modulation of gamma-radiation [3–5], RF collapse of the magnetic hyperfine structure [6], Rabi splitting of Mössbauer lines under NMR excitation [7–9], the effect of the rotating hyperfine magnetic field [10], gamma echo [11], etc. These phenomena noticeably enhance the efficiency of the Mössbauer effect as an experimental tool and allow getting information not attainable by conventional acquisition schemes. For

example, the modulation of Mössbauer spectra with ultrasound was efficiently used in studies of ultrasonic phenomena in solids [12]; RF collapse of the magnetic hyperfine structure was used in magnetic soft alloys for determination of the quadrupole splitting distribution [13]; Rabi splitting of Mössbauer lines were used to determine the amplitude of the RF field experienced by a nucleus and the hyperfine amplification factor [14]. It should be noted that the potential of modulation phenomena has not been exhausted; research in this direction is still ongoing.

Here we present a short overview of some experimental studies on new applications of Mössbauer effect using natural radioactive sources, carried out jointly at Kazan Federal University and Texas A&M University. Using these proofs of principal experiments as an example, we will show the potential application of the modulation effects for precise measurements of small displacements and quantum interference effects for photon shaping.

### *Application of the low-finesse $\gamma$ -ray frequency comb for high-resolution spectroscopy* [15]

It is common knowledge that the Mössbauer spectroscopy is one of the most precise spectroscopic methods for determining the energy shift of lines due to hyperfine interactions. The resolution of Mössbauer measurements is determined by the ratio of the resonance linewidth to the gamma resonance energy. For  $^{57}\text{Fe}$  nuclei, it is on the order of  $\sim 10^{-13}$ . The smaller this value, the more precisely we can investigate the interactions that lead to line shifts. In this regard, studies devoted to improving the resolution of gamma-resonance measurements are very interesting.

High-finesse frequency combs (HFC) with large ratio of the frequency spacing to the width of the spectral components have demonstrated remarkable results in many applications such as precision spectroscopy and metrology. Techniques using femtosecond-laser frequency combs allow to measure extremely narrow optical resonances with high resolution [16–19]. This is achieved by comparison of one of the spectral components of the calibrated frequency comb with the frequency of an extremely stable laser, which is tuned in resonance with the narrow absorption line under investigation. Enabling this technique in the  $\gamma$ -ray domain is expected to result in wide-range applications, such as more precise tests of astrophysical

models, quantum electrodynamics, and the variability of fundamental constants.

Special kind of  $\gamma$ -ray frequency combs can be generated by Doppler modulation of the radiation frequency, induced by mechanical vibrations of the source or a resonant absorber [2, 20-27]. These special  $\gamma$ -ray frequency combs with high finesse  $F \gg 1$ , where  $F$  is the ratio of the comb-tooth spacing to the tooth width, demonstrated that in many cases determination of small energy shifts between the source and absorber can be made more accurately in the time domain by transient and high-frequency modulation techniques than by conventional methods in frequency domain [24, 25, 28]. In time-domain-spectroscopy technique, the  $\gamma$ -ray frequency comb is transmitted through a single line absorber whose resonant transition is studied. Out of resonance the phase modulation of the field, generating the frequency comb, does not produce the modulation of the field intensity at the exit of the absorber. If one of the comb components comes to resonance with the absorber, the intensity of the transmitted radiation acquires oscillations. Their pattern is very sensitive to the resonant detuning. Here we show that a low-finesse comb (LFC) with  $F \ll 1$  is more sensitive to the small resonant detuning between the fundamental frequency of the radiation field and the absorber compared with the high-finesse comb (HFC).

We demonstrated LFC sensitivity in the experiments with the radiation source, which is a radioactive  $^{57}\text{Co}$  incorporated into rhodium matrix. The source emits 14.4-keV photons with the spectral width  $\Gamma_s = 1.13$  MHz, which is mainly defined by the lifetime of 14.4-keV excited state of  $^{57}\text{Fe}$ , the intermediate state in the cascade decay of  $^{57}\text{Co}$  to the ground state  $^{57}\text{Fe}$ . The absorber is a 25- $\mu\text{m}$ -thick stainless-steel foil with a natural abundance ( $\sim 2\%$ ) of  $^{57}\text{Fe}$ . Optical depth of the absorber is  $T_A = 5.18$ . The stainless-steel foil is glued on the polyvinylidene fluoride piezotransducer that transforms the sinusoidal signal from radio-frequency generator into the uniform vibration of the foil. The frequency and amplitude of the sinusoidal voltage were adjusted to have  $\Omega = 200$  kHz and  $a = 5.7$ , so that relation  $a\Omega \approx \Gamma_A$  was satisfied. The source is attached to the holder of the Mössbauer transducer causing Doppler shift of the radiation field to tune the source in resonance or out of resonance with the single line absorber. The time measurements were performed by means of the time-amplitude converter (TAC) working in the start-stop mode. The start pulses for

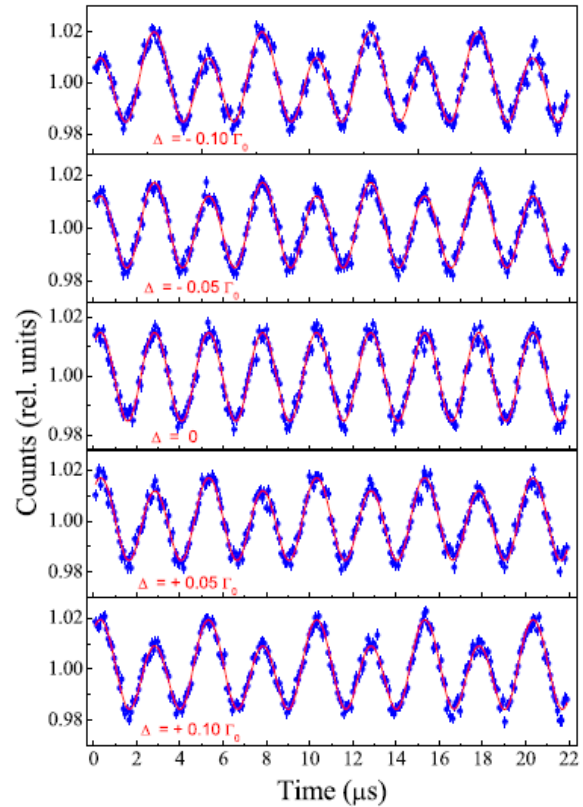


Fig. 1. Time dependence of the photon counts  $N(t)$  for different values of the resonant detuning. The number of counts is normalized to the mean value at exact resonance. The value of the detuning in units of  $\Gamma_0$  is indicated in each panel. The dots are experimental points and solid line is a theoretical fitting.

the converter were synchronized with radio-frequency generator and the stop pulses were formed from the signal of 14.4 keV  $\gamma$  counter at the instant of photon detection time.

The experimental results demonstrating the oscillations of the radiation intensity in time for different values of the resonant detunings are shown in Fig. 1. Time dependence of the number of counts is fitted to expression [15]:

$$N(t) = N_0 \sum_{n=0}^{\infty} D_n \cos[n\Omega(t - t_n)],$$

where  $N_0$  is the number of counts without absorber, and  $D_n$  and  $n\Omega t_n$  are the amplitude and phase of the  $n$ th harmonic. At exact resonance ( $\Delta = 0$ ), only even harmonics are not zero. Time delay of the second harmonic with respect to the vibration phase is  $t_2 = 61$  ns. This delay is caused by the contribution of dispersion, which produces a phase shift  $2\Omega t_2$ . The Fourier analysis of the oscillations allows to reconstruct the dependence of the ratio  $D_1 / D_2$  on  $\Delta$ , which is shown in Fig. 2, left panel. This dependence is compared with that for

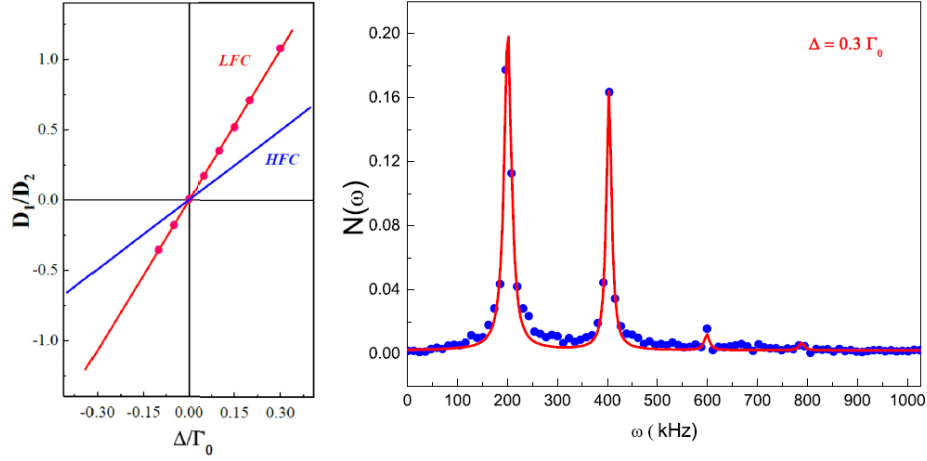


Fig. 2. (Left) Comparison of the dependence of  $D_1 / D_2$  on for LFC and HFC. Experimental data for LFC are shown by dots. (Right) Fourier content of the intensity oscillations for  $\Delta = 0.3\Gamma_0$ . Other parameters are defined in the text. Dots correspond to the data, obtained from the Fourier analysis of the experimentally observed intensity oscillations. Solid line is the analytical approximation by the set of Lorentzians.

HFC, generated by the vibration with high frequency  $\Omega = 10$  MHz and optimal value of the modulation index  $a = 1.08$ . We see that LFC is at least two times more sensitive to resonance than HFC since the slope of the dependence of  $D_1 / D_2$  on  $\Delta$  is two times steeper. Figure 2, right panel, shows the Fourier content of the oscillations of the radiation intensity for LFC when  $\Delta = 0.3\Gamma_0$ . The spectrum of these oscillations contains noticeable contributions of the first, second, and third harmonics. The width of these spectral components is defined by the length of the time window where the oscillations are measured. In our experiments, the spectral width of each Fourier component is close to 10 kHz. Thus we may conclude that within a moderate time of experiment the proposed method is able to measure the resonant detuning for  $^{57}\text{Fe}$  with the accuracy of 10 kHz, which is 100 times smaller than the absorption linewidth. This is essentially better accuracy than in the method, used in the gravitational red-shift measurements [29, 30], which employs four known values of the calibrated, controllable resonant detunings: two very large, comparable with the halfwidth of the absorption line, and two very small, comparable but appreciably exceeding the measured detuning. In time domain measurements, by extending considerably the length of the time window where the oscillations are collected, one can reach even higher accuracy of  $10^{-18}$  with a quite simple technique. In these experiments the regular signal grows as  $N$ , while the noise level rises as  $\sqrt{N}$ , where  $N$  is the number of detected photons. Therefore, to detect a very small

detuning, which gives a regular signal with the amplitude of 1%, we have to collect  $10^4$  counts in each time bin of our data acquisition system. This condition sets a limit on the accuracy of our method since experiments cannot last infinite time. The other technical limitations are well described in Refs. [29-31] and they are related to the stability of temperature and fine calibration of the mechanical parts of the experimental setup.

We demonstrate a method to measure precisely the resonant frequency of the absorber with LFC, with accuracy equal to a tiny fraction of the homogeneous absorption width. This method is also applicable in the optical domain. The modulation of the resonant frequency of atoms or impurity ions by Stark or Zeeman effects or the modulation of the frequency of the laser beam by an acousto-optical modulator are equivalent to the creation of a frequency comb in a particular reference frame. The interference of the scattered radiation field with the incident field is capable to produce the output intensity oscillations. By a proper choice of the modulation frequency and the modulation index, one can make these oscillations to be very sensitive to exact resonance or to measure the frequency difference between the incident radiation and the resonance frequency of atoms with the accuracy not limited by the value of the homogeneous linewidth.

***Application of the Mössbauer effect to the study of subnanometer harmonic displacements in thin solids*** [32]

Mössbauer spectroscopy offers a wide

range of applications due to very short wavelengths of  $\gamma$  photons and uniquely large ratios of the nuclear transition energy to the linewidth. Many Mössbauer experiments, valuable from the viewpoint of fundamental interest and applications, were reported since the invention of Mössbauer effect. Among them, we just briefly mention a few. They are gravitational red shift experiments [29-31, 33-36], novel tests of the general relativity theory [37, 38], detection of fast and tiny sample displacements induced by pulsed-laser heating [39] and other interesting effects. The gamma echo is generated if a thin absorber experiences a piston-like displacement equal to a half wavelength of gamma radiation, which is 43 pm for  $^{57}\text{Fe}$ . If this displacement is comparable or larger than the wavelength  $\lambda$  of  $\gamma$  radiation, the gamma echo exhibits several  $\gamma$ -radiation pulses each time when the absorber displacement reaches the value  $\lambda(n + 1/2)$ , where  $n$  is integer. Therefore we expect that  $\gamma$  echo could be used, for example, for calibrating the displacement of a scanning tunneling microscope. However, the intensity of  $\gamma$  echo is quite sensitive to the lateral distribution of the displacements of the absorber along the  $\gamma$  radiation beam. Therefore knowledge of the lateral displacement distribution, induced by piezoelectric transducer, is important. If we could apply  $\gamma$ -radiation for spatial measurements, then Angstrom resolution scale could be achieved. Moreover, the lateral distribution of the displacements of the vibrating absorber is quite important from the viewpoint of high-resolution spectroscopy with high and low-finesse frequency combs [15, 24, 25].

We will discuss the application of  $\gamma$  photons for subnanometer spatial measurements with subangstrom resolution for periodical displacements, induced by piezoelectric transducer. We expect that our results could be applied to calibrate also a step like displacements, controlled by  $\gamma$  echo. We employ 14.4-keV  $\gamma$  photons, emitted by radioactive  $^{57}\text{Co}$  with a wavelength 86 pm. Since we are not able to focus  $\gamma$ -radiation field and direct it to a desirable spot on the sample, we address to the spectral measurements. In our case, transmission spectra of the sample, containing resonant nuclei  $^{57}\text{Fe}$ , are proposed to be measured. We expect high depth resolution, while lateral resolution could be controlled by a lead mask with a small aperture, which could be moved along the surface of the sample. We expect that our method could provide

controllable and calibrated displacements of the surface with subangstrom resolution, which are produced by piezoelectric transducer oscillating with high frequency (several megahertz), low frequency (several kilohertz), or experiencing steplike displacement due to the applied step voltage.

In the method the sample containing resonant nuclei is mechanically vibrated. As a result, along with the main absorption line, a system of satellites appears in the spectrum, spaced apart at distances that are multiples of the vibration frequency. Line intensities of this comb structure are very sensitive to the vibration amplitude, which is extremely small (angstrom or even smaller). For the stainless steel foil, which is illuminated by  $\gamma$  radiation transmitted through a small aperture in the lead mask placed before the absorber, we measured displacements of the order of dozens of picometers with the accuracy of a few picometers. The influence of extremely small amplitude mechanical vibrations of the absorbers containing Mössbauer nuclei attracted attention since the invention of Mössbauer spectroscopy. Mössbauer sidebands, produced from a single parent line by absorber vibration, were observed in many different samples [2, 20-27, 40]. However, the intensity of the sidebands has not been yet satisfactory explained [23, 40]. There are two models of coherent and incoherent vibrations of nuclei in the absorber [20-23, 40]. Coherent model implies pistonlike vibration of the absorber with frequency  $\Omega$  and phase  $\psi$  along the propagation direction of  $\gamma$  quanta. This model predicts the intensity of the  $n$ th sideband proportional to the square of Bessel function  $J_n^2(m)$ , where  $m = 2\pi a_0/\lambda$  is the modulation index, which is proportional to the ratio of the amplitude  $a_0$  of the harmonic displacements  $a_z(t) = a_0 \sin(\Omega t + \psi)$  and the wave length  $\lambda$  of  $\gamma$  photon. The incoherent model, where phase  $\psi$  is assumed to be random and distributed with equal probability between 0 and  $\pi$ , was proposed by Abragam [41]. This model is based on the Rayleigh distribution of the nuclear-vibration amplitudes in the absorber, which predicts the sideband intensity proportional to  $e^{-m^2} I_n(m^2)$ , where  $I_n(m^2)$  is the modified Bessel function. However, both models or their combinations cannot describe perfectly all absorption spectra, which are experimentally observed for samples of different mechanical properties and chemical composition. To support this statement we refer to Chien and Walker who pointed out in Ref. [23] that “while unequivocally measured

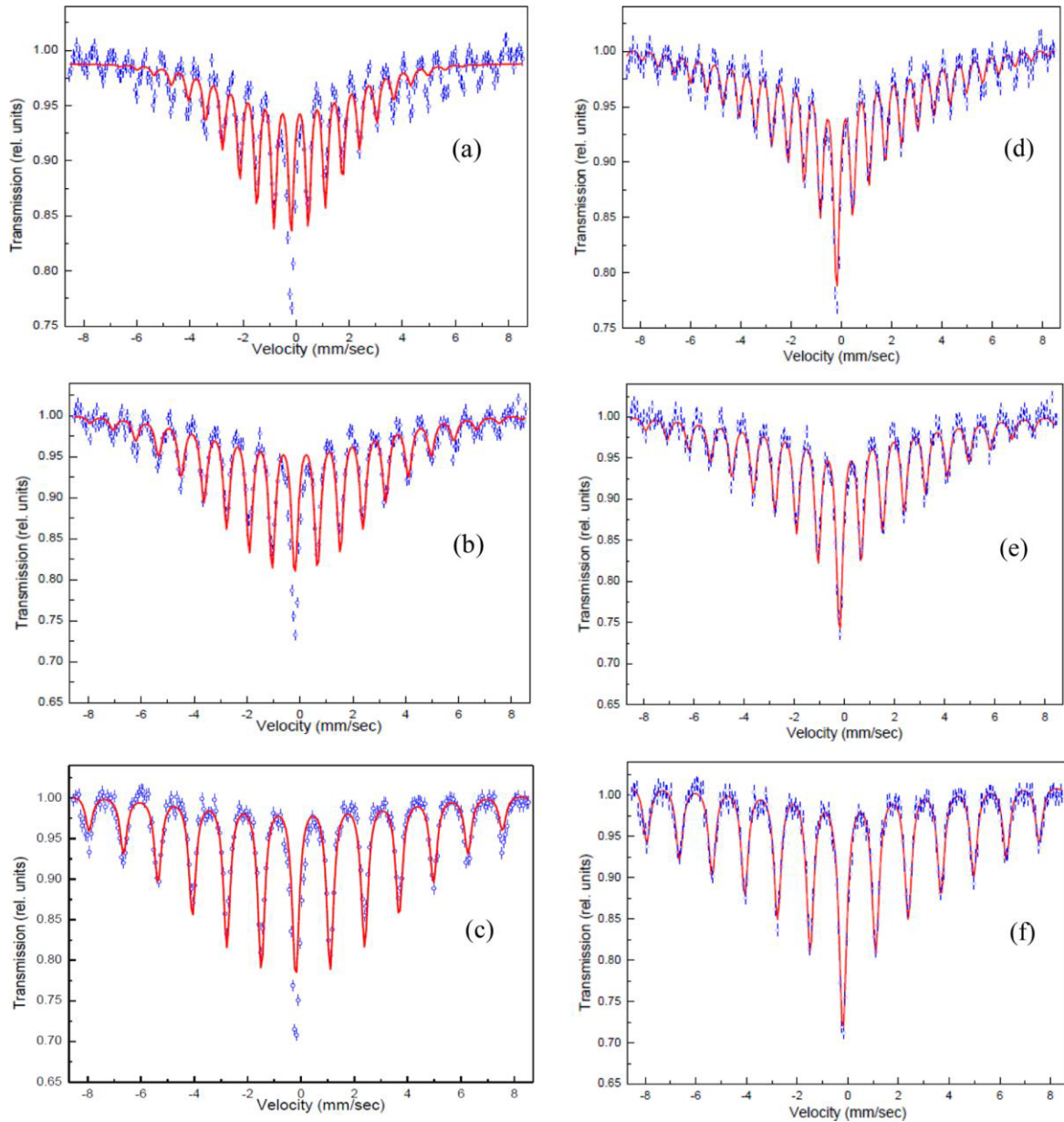


Fig. 3. Absorption spectra of the  $K_4Fe(CN)_6 \cdot 3H_2O$  powder absorber vibrated with the frequency  $\Omega$  equal to 7.5 (a) and (d), 10 (b) and (e), and 15 MHz (c) and (f). Dots are experimental data, solid line (in red) is the theoretical fitting to the Abragam model (a)–(c) and our model (d)–(f). For the Abragam model, the modulation index  $m_0 = 2\pi\sqrt{a^2}/\lambda$  is 3.42 (a), 3.66 (b), and 3.39 (c). For our model, we obtained  $m_0$ , which is 5.6 (d), 4.3 (e), and 4.7 (f).

intensities agree qualitatively with Abragam’s sideband theory, no existing theory at present can account quantitatively for the sideband intensities since the amplitude distribution that satisfactorily describes the data are not known at present.”

Fig. 3 shows our experimental spectra of the  $K_4Fe(CN)_6 \cdot 3H_2O$  powder absorber vibrated with the different frequency,  $\Omega$ . First, we made fitting of the experimental data to the Abragam model. The results are shown in Fig. 3, where in (a)–(c) the Abragam model is used, Abragam model gives bad fitting

except frequencies  $\Omega$  equal or higher than 35 MHz when we observed only three lines, i.e., the central component and two sidebands. For frequencies below 35 MHz, especially the central component and components near to it, are in a strong disagreement with the Abragam model. We modified the model to explain our experimental data. We propose a heuristic distribution of nuclear-vibration amplitudes, which is derived from the Gaussian distribution with appropriate modifications. The vibrations of nuclei in the absorber are supposed to be coherent, i.e., they have the

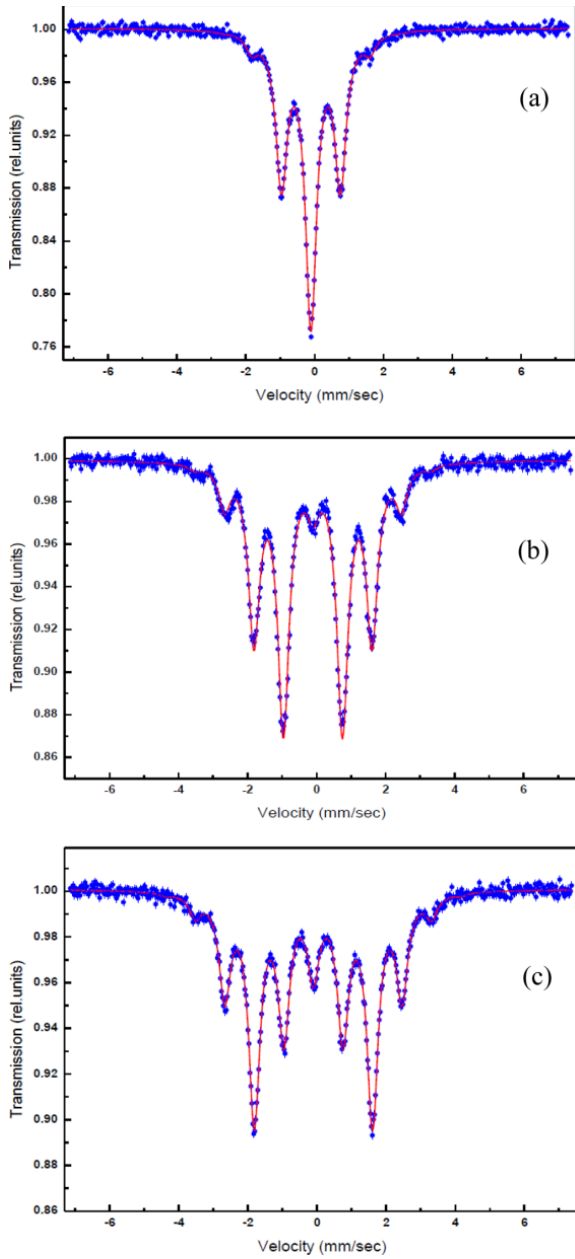


Fig. 4. Absorption spectra for stainless steel (SS) absorber vibrated with frequency 10 MHz. The applied voltage is 6.2 (a), 12.2 (b), and 15.4 V (c). Dots are experimental data, solid line (in red) is the theoretical fitting by our model. Fitting parameters are  $m_0 = 1.19$  and  $\sigma = 0.18$  (a),  $m_0 = 2.38$  and  $\sigma = 0.16$  (b), and  $m_0 = 3.01$  and  $\sigma = 0.16$  (c).

same phase  $\psi$ . Our model [32] provides good fitting of experimental spectra. The fitting results are shown in Fig. 3 (d–f) by solid red line. Depending on a parameter of the model  $\sigma$ , the proposed distribution tends to the Rayleigh distribution inherent to the incoherent model if  $\sigma \rightarrow 0.72$ , or it tends to a delta distribution, inherent to the coherent model if  $\sigma \rightarrow 0$  (see Fig. 4). For powder, the distribution of the powder-grain displacements, obtained from

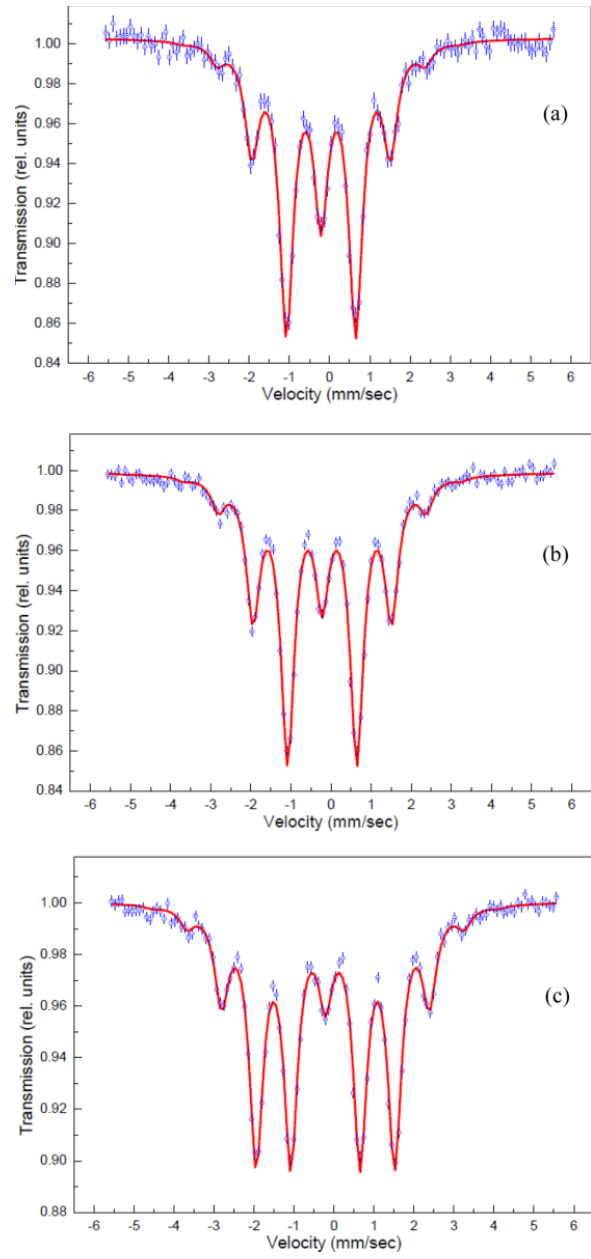


Fig. 5. Absorption spectra for the SS absorber obtained with the lead mask. Diameter of the hole in the lead mask is 2.45 (a), 1.7 (b), and 1.1 mm (c). The absorber is vibrated with frequency 10.7 MHz. Dots are experimental data, solid line (in red) is the theoretical fitting to our model. The values of the modulation index  $m_0$  and parameter  $\zeta$  are 1.85 and 0.27 (a), 2.08 and 0.25 (b), and 2.68 and 0.21 (c), respectively.

the spectrum fitting, is close to the continuous uniform distribution with wide scattering of the vibration amplitudes, which is very different from the Rayleigh distribution. For stainless steel foil, we found that the displacement distribution along the surface of a thin foil is close to the narrow, bell-shape distribution. Physical interpretation of these results is



discussed. For SS foil, we experimentally verified our conclusions placing a lead mask just in the front of the absorber. We made an aperture in the lead mask and compared the observed Mössbauer spectra with our theoretical predictions. We observed a change of Mössbauer spectra with decrease of the size of the aperture, supporting firmly our model. The absorption spectra of the absorber with the lead mask are shown in Fig. 5. Diameter of the hole in the mask was varied from 2.45 to 1.1 mm. These spectra are obtained for the same frequency and voltage of the RF generator. In the coherent model the central component becomes zero for the modulation index  $m = 2.4$ . We suppose that spectra in Fig. 5 are obtained with the modulation index quite close to this value. Therefore the observed lessening of the central component of the absorption spectra with diminution of the hole diameter in the lead mask proves that scattering of the vibration amplitudes of nuclei, exposed to  $\gamma$  radiation, becomes smaller with decreasing size of the hole. At the same time the relative intensities of the sidebands increase with diminution of the hole diameter.

Our measurements show that the Mössbauer effect can be used to measure the amplitude of subnanometer harmonic displacements of the absorber with an accuracy of less than half angstrom. So, for example, analysis of the spectra shown in Figs. 5 (a) and (c) reveals for the smallest hole in the lead mask the maximum value of the vibration amplitude is  $a_0 = 36.7$  pm at the disk center, while for the edge of the hole it is about 34.7 pm. Last one differs from  $a_0$  only by 2 pm. This 5% difference gives the accuracy of the displacement measurement with the smallest hole.

#### ***Application of the Mössbauer effect to the topographic study of ultra-small displacements of the surface [42]***

We performed also a set of experiments using a lead mask with a hole of 0.6 mm in diameter. A special holder with a micrometer screw gauge was designed, which made it possible to change the position of the hole along the surface of the absorber with a step of about 10  $\mu\text{m}$ . The mechanical part of the experimental setup is described in [42]. Scanning of the surface of the absorber made it possible to map the displacements of the sections of the stainless steel foil vibrating with a frequency of 10.2 MHz at a fixed RF generator voltage of 10 V. Fig. 6 shows a map

of the displacements along the surface of the foil with its center at  $x = 0$ . The displacement amplitude is proportional to the found modulation index  $m$ . The standard deviation of the oscillation amplitudes was 3.6 pm at the center and 6.6 pm at the edges of the foil.

The topography of ultra-small displacements of the surface of a thin oscillating sample has been carried out for the first time using the Mössbauer spectroscopy. It has been established that the method allows measuring the amplitude of subangstrom mechanical displacements of the surface with accuracy an order of magnitude higher than the diffraction limit. The method we developed can be used to calibrate the absolute shifts of the tip of a scanning tunneling microscope. The measured tunneling current in the scanning tunneling microscope usually makes it possible to estimate the absolute value of the microscope tip displacement if the local density of states of the test substance is known. Our method allows creating calibrated displacements of a smooth surface, which can be coated with a thin (micron or thinner) layer of the test substance that does not violate the mechanical properties of the (foil-piezoelectric transducer) assembly. Then, the local density of states of the test substance can be accurately determined by comparing the STM tunneling current with the calibrated displacements measured by our method.

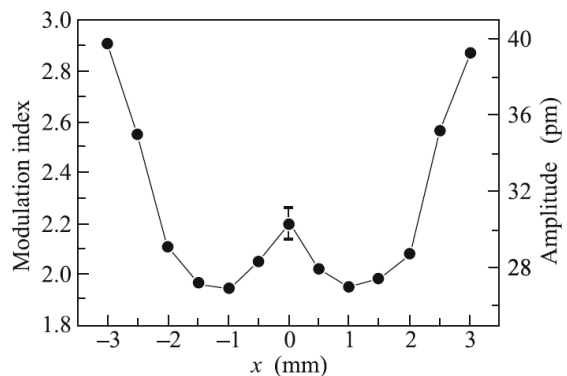


Fig. 6. (Left vertical axis) Modulation index and (right vertical axis) corresponding displacement amplitude versus the position of the hole in the lead mask, which moved along the surface of the stainless steel foil with the center at  $x = 0$ .

#### ***Application of the Mössbauer effect to the study of opto-acoustic phenomena [39].***

Let's consider how the effects induced by pulsed laser radiation manifest themselves in Mössbauer measurements. When a pulsed laser beam is incident on the surface of a solid at the thermo elastic regime, various characteristic elastic waveforms can be excited, depending

strongly not only on optical penetration, thermal diffusion, elastic and geometrical features of the materials, but also on the parameters of the exciting laser pulse including its shape, focus spot, and pulse width. The action of high-intensity pulsed optical radiation on matter produces strong thermal and hydrodynamic disturbances of the equilibrium state of the medium, which are accompanied by the excitation of sound [43]. For moderate densities of released-energy in the medium the main factor contributing to the process of sound generation is usually the thermal expansion of the light-absorbing volume of the matter. There are other mechanisms of the optical generation of ultrasonic waves, tunable up to several GHz and more, for example, using crossed laser pulse excitation [44]. The detection of light-induced ultrasonic signals allows getting valuable information about physical properties of materials, dynamics of light induced phase transitions and even dynamics of photo induced chemical reactions. Acoustic signals are usually measured using piezoelectric detectors, optical detection schemes, induction coils, etc. Until now Mössbauer technique has been never used for study the ultrasonic oscillations induced by the opto-acoustic effect. In the previous experiments, the ultrasonic modulation of Mössbauer radiation was preferably induced by vibrations excited by radio-frequency field via piezoelectric or magnetostriction effects. At the same time, extremely useful features of Mössbauer effect allow to hope that it could be effectively used for study the acoustic oscillations induced in materials by pulsed laser radiation. Extremely high selectivity of  $\gamma$ -resonance (up to  $10^{-13}$ – $10^{-15}$ ) and extremely short wavelength of Mössbauer radiation ( $\lambda < 1\text{Å}$ ) make it possible to observe the vibrations of Mössbauer nuclei in different crystallographic positions and determine small displacements of atoms with an accuracy of no less than  $\lambda/2$ . For example, even so tiny displacements of  $^{57}\text{Fe}$  or  $^{67}\text{Zn}$  nuclei by 0.43 and 0.066 Å, respectively, are sufficient for the transition from destructive to constructive interference between the incident and scattered forward resonance radiation due to the phase shift by  $\pi$  [24, 25, 28, 45] and to change dramatically the shape of the photon wave passing through the resonant medium. So, the accuracy of gamma optics exceeds the accuracy of optical measurements at least by three orders of magnitude.

The experiment was performed in the transmission geometry with a  $^{57}\text{Co}$  source in a

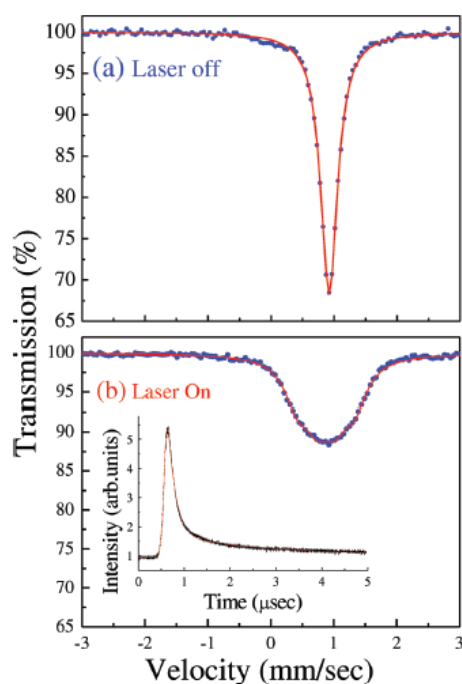


Fig. 7. Mössbauer spectra of the MgO:Fe sample (a) without the laser action and (b) under the laser excitation. The inset shows the shape of the laser pulse.

rhodium matrix and an  $\text{MgO}:\text{}^{57}\text{Fe}^{2+}$  plate as an absorber. Thin plates of MgO single crystals obtained from MTI Corporation, with the axis orientation  $\langle 100 \rangle$ , were doped by  $^{57}\text{Fe}$  atoms using thermal diffusion. The optical absorption spectrum of our sample consists of the broad optical absorption bands of iron ions in the region of 530 and 600 nm. The first band coincides with the wavelength of commercial lasers (532 nm), and this transition can be used for the sound generation in the sample under investigation. The optical excitation was performed by means of the pulsed Nd:YAG laser (Verdi V18, Coherent) working in the frequency doubling mode (532 nm) of the main laser harmonic. Fig. 7 shows the Mössbauer spectrum of the unexcited  $\text{MgO}:\text{}^{57}\text{Fe}^{2+}$  sample and the spectrum obtained under the action of the pulsed laser radiation with power of 1.85W and the repetition rate of 10 kHz. It can be seen that optical radiation leads to considerable broadening of the absorption line. The observed broadening is connected with manifestation of the opto-acoustic effect in Mössbauer spectrum. The absorption of the laser radiation by the sample and subsequent relaxation leads to the deformation of the crystal lattice and excitation of the acoustic vibrations.

It is known that the amplitudes of the opto-acoustic signals are proportional to the variable part of the light flux. In this work, the

acoustic waves were excited by the exponential laser pulses with a decay constant of  $\sim 160$  ns (see inset in Fig. 7). The rectangular sample ( $\text{MgO}:\text{}^{57}\text{Fe}^{2+}$  plate) was fixed in a lead holder so that characteristic mechanical modes could be induced in it under optical excitation. Under these conditions, the frequency of the main harmonic of the mechanical vibrations of the plate is proportional to

$$\Omega = C \cdot c_1^2 h \cdot \left[ (1/a)^2 + (1/b)^2 \right],$$

where  $c_1$  is the longitudinal speed of sound,  $a$  and  $b$  are the transverse dimensions of the plate,  $h$  is the thickness of the plate, and  $C$  is the coefficient determined by the plate fixation conditions [46]. The vibrations of nuclei with the frequency  $\Omega$  are revealed in Mössbauer spectra in the form of a set of symmetric satellites displaced from the central unshifted component by  $\pm n\hbar\Omega$ , where  $n$  is integer number. The amplitudes of the satellites depending on modulation index  $m$  are determined by Bessel functions of the first kind,  $J_n^2(m)$ , in the case of coherent vibrations of all nuclei with same amplitude and by modified Bessel functions,  $e^{-m^2} I_n(m^2)$ , when the amplitude of the vibrations is distributed according to the Rayleigh distribution function. If the frequency of the nuclear vibrations is smaller than the natural linewidth of the resonance transition  $\Gamma_0$  (for the  $^{57}\text{Fe}$  nuclei  $\Gamma_0 \approx 1.1\text{MHz}$ ), then the radiation modulation is manifested in Mössbauer spectra as the line broadening only (Fig. 7). This considerably reduces the statistical accuracy of determination of the frequency and amplitude of the nuclear vibrations induced by the laser radiation. In this case, time domain measurements of the number of gamma photons, transmitted through the sample, as a function of time, elapsed after the excitation of the sample by the laser pulse, are much more informative.

The scheme of an experimental setup is shown in Fig. 8. The time measurements were performed by means of the time–amplitude converter (TAC) working in the start–stop mode. The start pulses for the converter were formed from the signal of a photo-diode (PhD) at the time of the laser excitation and the stop pulses were formed from the signal of 14.4 keV gamma counter at the instant of photon detection time. A detailed description of the experimental setup is given in [47].

Figs. 9 and 10 show the time dependences of the normalized radiation intensity transmitted through the vibrating absorber under the pulsed

laser excitation ( $\lambda = 532$  nm). Fig. 9a shows the time spectrum obtained during the movement of the source with constant velocity detuned from the resonance by  $\Delta\omega = \omega_a - \omega_s = 2\Gamma_0$ . The spectrum shown in Fig. 10a was recorded at resonance of the source radiation line with the absorption line of the sample,  $\Delta\omega = 0$ . These dependences have a strictly periodic character. This makes it possible to determine the parameters of the nuclear vibrations with high accuracy by fitting of the experimental time domain spectrum to the theoretical curve. The points in Figs. 9b and 10b, connected by thin dark lines, show the result of the Fourier analysis of the experimental spectra presented in Figs. 9a and 10a, respectively.

The best fit between theory and experiment for the time spectra, given in Figs. 9a and 10a, was obtained when  $\Omega = 221$  kHz and  $a = x_0 / \lambda = 16$ . The  $\Omega$  value agrees well both with the frequency of the main harmonic of the characteristic mechanical vibrations of the studied plate, defined by the above expression, and with the frequency of the main peak of the Fourier component of the time spectrum recorded with the detuning from the resonance by  $\Delta\omega = 2\Gamma_0$  (Fig. 9b). For determining the amplitudes of the nuclear vibrations we can use also the ratio of amplitudes of the Fourier expansion components of the time spectrum. The ratio of the even Fourier harmonics shown in Fig. 10b is equal to 0.43. This ratio  $D_{4\Omega} / D_{2\Omega}$  of the even Fourier harmonics corresponds to a modulation index value of  $\sim 16$ , which is in good agreement with the value found by fitting

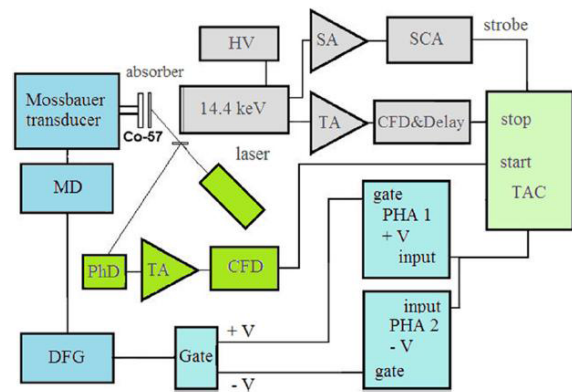


Fig. 8. Scheme of the experimental setup: TAC – time–amplitude converter, PHA – pulse–height analyzer, PhD – photodiode, CFD – constant ratio discriminator, SCA – single channel analyzer, TA – time amplifier, SA – spectrometric amplifier, HV – high–voltage source, MD – Mössbauer drive system, and DFG – signal generator.

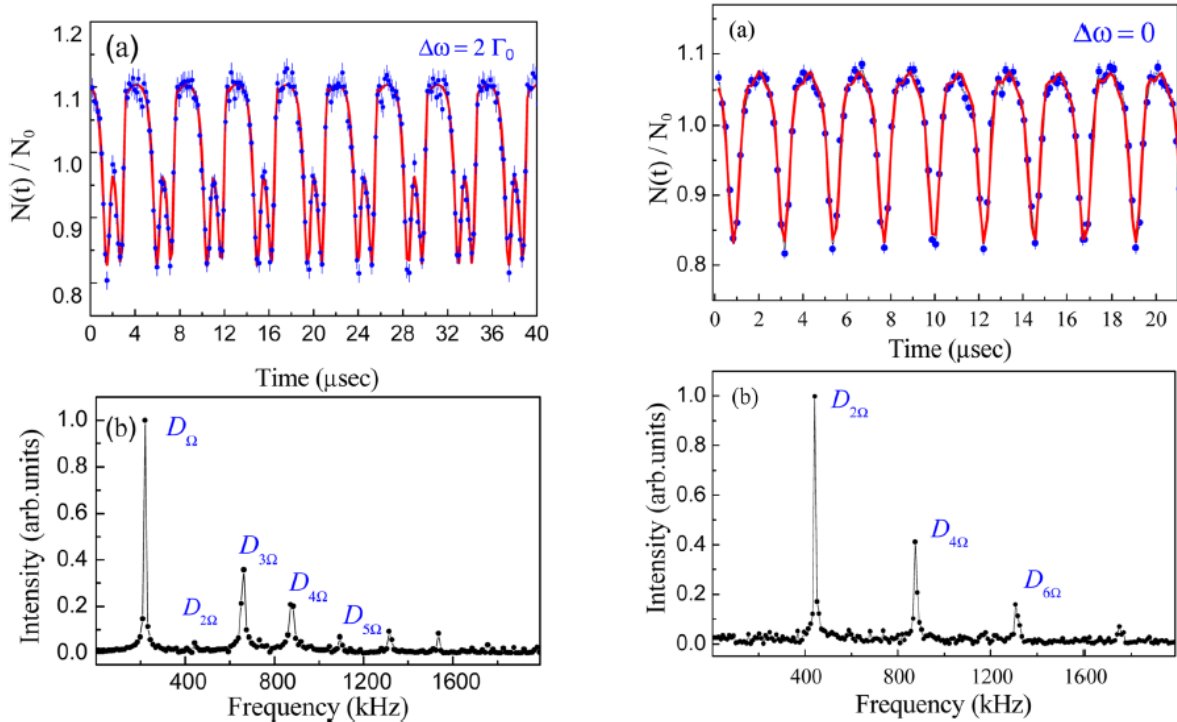


Fig. 9. (Left) (a) Time dependence of the normalized intensity of the transmitted  $\gamma$ -radiation and (b) its Fourier spectrum under the excitation of the MgO:Fe absorber by the pulsed laser radiation with a power of 1.85 W. Detuning from the resonance is  $\Delta\omega = 2\Gamma_0$ . The solid red line is the fit of the experimental spectrum; are the Fourier harmonics of the time spectrum.

Fig. 10. (Right) (a) Normalized time spectrum of the transmitted  $\gamma$ -radiation intensity under the laser excitation of the absorber, and (b) Fourier spectrum of the time spectrum. The source radiation is in exact resonance with the absorption line of the sample ( $\Delta\omega = 0$ ). The solid line is the fit of the experimental spectrum to the theoretical expression (4) given in [39].

the experimental time spectrum (Fig. 10a).

The suggested method to use Fourier decomposition and the ratio of its even harmonics allows easy determination of the amplitudes of the nuclear vibrations induced by pulsed laser excitation. To demonstrate the main features of proposed scheme in a clear and simple way, experiment was performed under conditions when only the characteristic mechanical modes of the plate can be induced by the laser pulses. It should be noted that this method can also be useful for studying more complex opto-acoustic and magneto-elastic interactions induced by the laser radiation. The detection of the acoustic signals makes it possible to obtain valuable information about the physical properties of the studied objects and/or laser-induced processes. Acoustic waves can be measured by piezoelectric detectors, using optical schemes, induction coils for magnetic materials, etc. In the optical schemes the information is mainly obtained from the surface manifestations of the magneto-elastic

interactions. In the induction schemes the electromotive force signal is obtained from the coil and this signal is proportional to the rate of change of the magnetic induction flux through the coil. Therefore, the detected signal in induction method is averaged over all magnetic sublattices existing in the material under study [48]. Undoubtedly, the method suggested above would make it possible to extend the experimental possibilities to studying magnetic materials with several magnetic sublattices since oscillations of each sublattice can be studied in this case separately by means of tuning the emission line of the source to the absorption line corresponding to the individual sublattice under study. Our method can be useful in studying the dynamics of magneto acoustic waves in complex magnetic crystals with the pronounced acoustic anharmonicity nascent due to the high intensity pulsed laser radiation, which allows to reach rather high deformations and clearly observe nonlinear processes in the samples.

## Conclusion

The above results demonstrate once again the versatility of the Mössbauer effect and how wide the scope of its application can be. We are sure that even more interesting applications of the Mössbauer effect will emerge thanks to the Mössbauer community, and we hope that with this brief, humble description, we will stimulate the search for new applications.

## References

- [1] J. K. Srivastava, in: *Advances in Mössbauer Spectroscopy*, edited by J. K. Srivastava (Elsevier, Amsterdam, 1983), p. 761.
- [2] S. L. Ruby and D. I. Bolef, *Phys. Rev. Lett.* **5** (1960) 5.
- [3] N. D. Heiman, L. Pfeiffer, and J. C. Walker, *Phys. Rev. Lett.* **21** (1968) 93.
- [4] N. D. Heiman, L. Pfeiffer, and J. C. Walker, *J. Appl. Phys.* **40** (1969) 1410.
- [5] L. Pfeiffer, N. D. Heiman, and J. C. Walker, *Phys. Rev. B* **6** (1972) 74.
- [6] L. Pfeiffer, *J. Appl. Phys.* **42** (1971) 1725.
- [7] F. G. Vagizov, *Hyperfine Interact.* **61** (1990) 1359.
- [8] I. Tittonen, M. Lippmaa, E. Ikonen, et al. *69* (1992) 2815.
- [9] F. G. Vagizov, *Hyperfine Interact.* **95** (1995) 85.
- [10] F. G. Vagizov, R. A. Manapov, E. K. Sadykov, et al. *Hyperfine Interact.* **116** (1998) 91.
- [11] P. Heliö, I. Tittonen, M. Lippmaa, et al. *Phys. Rev. Lett.* **66** (1991) 2037.
- [12] M. Kopcewicz, in: *Mössbauer Spectroscopy Applied to Inorganic Chemistry*, edited by G. F. Long and F. Gradjean (Plenum Press, New York, 1989), chap. 5, p. 243.
- [13] M. Kopcewicz, H. G. Wagner, and U. Gonser, *Solid State Commun.* **48** (1983) 531.
- [14] F. G. Vagizov, *Hyperfine Interact.* **61** (1990) 1363.
- [15] R. N. Shakhmuratov, F. G. Vagizov, Marlan O. Scully et al. *Phys. Rev. A* **94** (2016) 043849
- [16] Th. Udem, R. Holzwarth, and T. W. Hansch, *Nature*, **416**, 233 (2002).
- [17] S. T. Cundiff and J. Ye, *Rev. Mod. Phys.* **75**, 325 (2003).
- [18] T. W. Hansch, *Passion for Precision*, Nobel lecture, December 8, 2005.
- [19] J. L. Hall, *Defining and Measuring Optical Frequencies: the Optical Clock Opportunity - and More*, Nobel lecture, December 8, 2005.
- [20] T. E. Cranshaw and P. Reivari, *Proc. Phys. Soc.* **90**, 1059 (1967).
- [21] G. Kornfeld, *Phys. Rev.* **177**, 494 (1969).
- [22] J. Mishroy and D. I. Bolef, *Mössbauer Effect Methodology*, edited by I. J. Gruverman (Plenum Press, Inc., New York, 1968), Vol. 4, pp. 13–35.
- [23] C. L. Chein and J. C. Walker, *Phys. Rev. B* **13**, 1876 (1976).
- [24] G. J. Perlow, *Phys. Rev. Lett.* **40**, 896 (1978).
- [25] J. E. Monahan and G. J. Perlow, *Phys. Rev. A* **20**, 1499 (1979).
- [26] S.L. Popov, G.V. Smirnov, Y. V. Shvyd'ko, *Pis'ma Zh. Eksp. Teor. Fiz.* **49**, 651 (1989)
- [27] Yu. V. Shvyd'ko and G. V. Smirnov, *J. Phys.: Condens. Matter* **4**, 2663 (1992).
- [28] P. Helistö, E. Ikonen, T. Katila, W. Potzel, and K. Riski, *Phys. Rev. B* **30**, 2345 (1984).
- [29] T. E. Cranshaw and J. P. Schiffer, *Proc. Phys. Soc.* **84**, 245 (1964).
- [30] R. V. Pound and J. L. Snider, *Phys. Rev.* **140**, B788 (1965).
- [31] W. Potzel, C. Schafer, M. Steiner, et al. *Hyperfine Interact.* **72**, 195 (1992).
- [32] R. N. Shakhmuratov, F. G. Vagizov, *Phys. Rev. A* **95** (2017) 245429.
- [33] T. E. Cranshaw, J. P. Schiffer, and A. B. Whitehead, *Phys. Rev. Lett.* **4**, 163 (1960).
- [34] R. V. Pound and G. A. Rebka, *Phys. Rev. Lett.* **4**, 337 (1960).
- [35] R. V. Pound and J. L. Snider, *Phys. Rev. Lett.* **13**, 539 (1964).
- [36] T. Katila and K. J. Riski, *Phys. Lett. A* **83**, 51 (1981).
- [37] Y. Friedman, E. Yudkin, I. Nowik, et al. *J. Synchrotron Radiat.* **22**, 723 (2015).
- [38] Y. Friedman, I. Nowik, I. Felner, et al. *Europhys. Lett.* **114**, 50010 (2016).
- [39] F. Vagizov, R. Shakhmuratov, E. Sadykov, *Phys. Status Solidi B* **252** (2015) 469.
- [40] A.R. Mkrtychyan, G.A. Arutyunyan, et al. *Phys. Status Solidi B* **92** (1979) 23.
- [41] A. Abragam, *C. R. Acad. Sci.* **0250**, 4334 (1960).
- [42] R. N. Shakhmuratov, F. G. Vagizov, *JETP Letters*, **108** (2018) 772.
- [43] J. F. Ready, *Effects of High-Power Laser Radiation*, Academic Press, New York, 1971.
- [44] K. A. Nelson, D. R. Lutz, M. D. Fayer, L. Madison, *Phys. Rev. B* **24**, 3261 (1981).
- [45] G. J. Perlow, W. Potzel, R. M. Kash, and H. De Waard, *J. Phys. (Paris)* **35**, C197 (1974).
- [46] L. D. Landau and E. M. Lifshitz, *Course of Theoretical Physics*, Vol. 7, Pergamon, New York, 1986, chap. 1.
- [47] R. N. Shakhmuratov, F. Vagizov, J. Odeurs, et al. *Phys. Rev. A* **80**, 063805 (2009).
- [48] D. L. Dorofeev, G. V. Pakhomov, and B. A. Zon, *Phys. Rev. E* **71**, 026607 (2005).